Dependence of Chalcogenide Glassy $Bi_x(As_2S_3)_{100-x}$ System Optical Parameters on the Doping Content

M.V. Šiljegović[a,*], S.R. Lukić-Petrović[a], D.D. Štrbac[b], N. Ćelić[a] and I.R. Videnović[c]

[a]University of Novi Sad, Faculty of Sciences, Trg Dositeja Obradovića 4, 21000 Novi Sad, Serbia

[b]University of Novi Sad, Faculty of Technical Sciences, Trg Dositeja Obradovića 6, Novi Sad, Serbia

[c]University of Belgrade, Faculty of Physics, Studentski trg 12, 11000 Belgrade, Serbia

(Received October 18, 2017)

In this paper we present the results of optical and spectral characteristics of the quasibinary glassy system Bi–As_2S_3. From the obtained spectra we determined the optical band gap and the level of structural disorder for different doping atoms content. The decrease of the optical gap with increase on Bi atoms content was discussed in terms of chemical composition and arrangement of structural units, using the Raman spectroscopy results. The Wemple–DiDomenico model was used to describe the refractive index behavior and correlations between linear and nonlinear optical quantities of investigated chalcogenides, yielding significant parameters for the structural analysis. Having obtained high values of nonlinear refractive index, potential applications of these materials in telecommunication systems are discussed.

DOI: 10.12693/APhysPolA.134.498

PACS/topics: glasses, absorption spectra, Raman spectra, refractive index

1. Introduction

Chalcogenide glasses exhibit excellent transmission in the near and far infrared spectral region. They are high refractive index materials with a nonlinear refractive index typically 100 times greater than that of silica, especially those containing heavy metal elements [1, 2]. For these reasons chalcogenide glasses have been studied for ultrafast switching in telecommunication systems [3]. These glasses also have the advantage of high chemical and thermal stability, which allows production of easy-to-prepare optical devices [4–6]. Furthermore, their photosensitivity and a possibility to modify the refractive index of the glass in a controlled manner, provide promising technique for obtaining channel waveguides [7, 8], bypassing the standard photolithographic processes. Therefore, the design and production of optical components based on chalcogenide glasses require detailed information on their optical properties over a range of wavelengths.

In this paper, we focus our study on some optical and spectral characteristics of quasibinary $Bi_x(As_2S_3)_{100-x}$ glassy system. We studied the changes in optical band gap E_g and correlated it to the content of doping atom in arsenic-sulphide matrix. The Raman spectra analysis enabled the determination of particular structural units that have the most significant impact on material properties.

In addition, the aim of this work was to study linear and nonlinear optical properties of these glasses. In order to establish a correlation between the linear and nonlinear optical quantities, the Wemple–DiDomenico (WDD) model was applied for refractive index dispersion analysis. The obtained results were interpreted from the viewpoints of structural modification of the amorphous matrix due to doping with Bi atoms, and their practical applications.

2. Experimental

The synthesis of chalcogenide glasses of quasibinary $Bi_x(As_2S_3)_{100-x}$ system (x = 1.5, 3, 5, and 7 at.% Bi) was performed by the method of cascade heating, according to the regime described in the previous publication [9]. These compositions are selected with regard to the amorphous region boundaries on the phase diagram. To enable recording transmission spectra, glass samples with x = 1.5, 3, and 5 at.% Bi were mechanically processed with abrasive powders of different grain sizes to form planparallel plates of about 0.7 mm in thickness, and polished to a high gloss to avoid diffuse scattering effects. Transmission measurements were carried out using NIR Perkin-Elmer spectrophotometer model Lambda-950 in the wavelength interval of 400–2500 nm. The opacity of the glass with the highest content of doping atoms in this spectral region has prevented the spectral analysis for this sample. The refractive index dispersion was measured by the direct method of prism using a laboratory-constructed setup [10]. The prisms were prepared from the selected pieces of glass samples by mechanical treatment and polishing. The angles of prisms were measured by two-circle optical Enraf Nonus Y-881 goniometer with the accuracy of 2′. The Raman spectra were recorded at room temperature, using confocal Raman imaging system alpha 300 R (WITec) with the doubled Nd:YAG laser (532 nm) and in a backscattered geometry.

3. Results and discussion

The transmission spectra were used to determine the absorption coefficient α of the investigated glasses, according to the equation

*corresponding author; e-mail: mirjana.siljegovic@df.uns.ac.rs

$$\alpha = \frac{1}{d} \ln \frac{1}{T} \tag{1}$$

where d is the sample thickness.

The Vis-NIR absorption spectra are shown in Fig. 1. According to Eq. (1), thickness of the samples has a significant impact on the absorption coefficient value. However, during the preparation it was not possible to achieve absolutely the same thickness for all the samples. Therefore, a small difference between the thickness values exists, as indicated in Fig. 1 and may have certain consequences on the discussion of the optical characteristics of the analyzed materials.

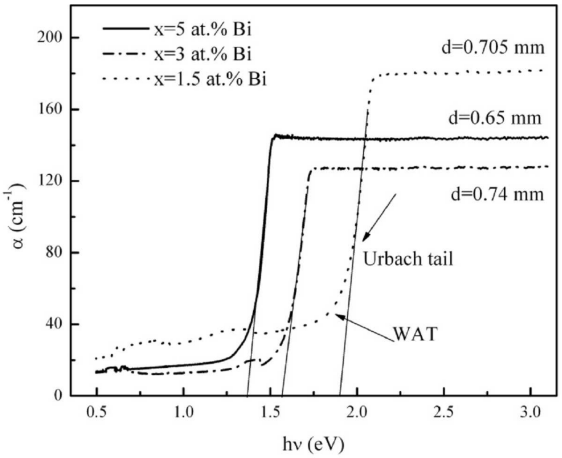

Fig. 1. Dispersion curves of absorption coefficient of glassy $Bi_x(As_2S_3)_{100-x}$ system.

In the high-energy region of the spectrum one observes two characteristic slopes. The steeply sloped line corresponds to the Urbach tail and the gradually sloped line corresponds to the weak absorption tail (WAT). It should be noted that part of the spectra corresponding to the Urbach tail is similar in different materials, while the WAT is a structure-sensitive property [11]. Therefore, WAT characterizes the loss factors in chalcogenide glasses [12] and is induced by additional band-gap states. Figure 1 also shows that the WAT amplitude is the highest for the sample with minimum content of Bi. The tail absorption originates in weak transitions between localized states deep in the gap and the extended states in the conduction band (or valence band), which can be expressed by the following equation [11]:

$$\alpha(\omega) = \frac{\pi^2 e^2 \hbar^2}{mc} \frac{f}{n} \int_{(\hbar\omega_{\max} - \hbar\omega)}^{\infty} V(E_i)\, N(E_i)\, g(\hbar\omega - \hbar\omega_{\max} + E_i)\, \mathrm{d}E_i, \tag{2}$$

where e, m, c and n represent the electronic charge, mass of electron, velocity of light, and refractive index, respectively, f is the oscillator strength, $\hbar\omega_{\max}$ is the maximum optical transition energy in the tail absorption, $V(E)$ is the volume of the localized states in glass, $N(E)$ is the density of the localized states, and $g(E)$ represents the state density of the opposite extended states in the transition process.

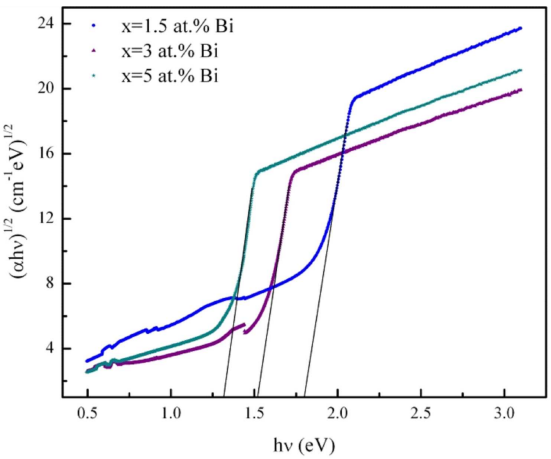

Fig. 2. Dependence of $(\alpha h\nu)^{1/2}$ on $h\nu$ of glassy $Bi_x(As_2S_3)_{100-x}$ system.

In this interpretation WAT is associated with the deep potential fluctuations which may occur due to disorder, defects, or impurities [11]. Thus, increased tail absorption in glass with $x = 1.5$ at.% Bi, compared to the glasses with $x = 3$ and 5 at.% Bi is induced either by the high value of $N(E)$ or by the high transition probability of the localized states. Another feature of the recorded absorption spectra is the red shift of the optical absorption edge as a function of dopant atoms content.

TABLE I

Values of the optical band gap and width tails of the localised states for the samples of $Bi_x(As_2S_3)_{100-x}$ system.

x [at.%]	E_g [eV]	E_e [meV]
1.5	1.80 (4)	144.3 (7)
3	1.53 (3)	90.5 (2)
5	1.32 (2)	86.7 (2)

The direct optical band gap E_g values are determined from the plots of $(\alpha h\nu)^{1/2}$ as a function of $h\nu$, by the extrapolation of the linear part of the curve (Fig. 2). The obtained values are given in Table I.

The E_g values indicate decreasing trend of the parameter E_g with increased doping atoms content. Recalling the optical band gap value of As_2S_3 glass of 2.35–2.40 eV [13], it may be noticed that the presence of small amount of Bi atoms (1.5 at.%) significantly reduces this parameter. Further on, the decrease of E_g with increase of dopant content can be approximated by a linear function. The significant red shift of the absorption edge can be explained either by increasing the length of As–S bonds without any particular changes in the structure or by dependence of the width of the localized states near the edge of mobility on disorder in the glass matrix [14]. Namely the existence of the defect structural units in the tails broadens the energy level of the tail band and narrows the optical gap [15, 16].

The slope of the linear part in the area of the Urbach tail in Fig. 1 represents the width of the band tail due to the presence of the localised states described by the parameter E_e [17] and enables further analysis of the parameter E_g. The parameter E_e is determined from the slope of the linear part of the plot $\ln\alpha = f(h\nu)$, according to the relation

$$\alpha = \alpha_0 \exp \frac{\hbar\omega}{E_e}. \tag{3}$$

The obtained values are shown in Table I.

Slightly higher slope of the linear part of the $\ln\alpha = f(h\nu)$ curve, illustrated in Fig. 3, can be noticed only for the sample with a minimum content of Bi. For other two samples these slopes are almost the same, see E_e values in Table I. Considering the E_e value of 81 meV for the undoped glass [18], one may conclude that the largest effect on disorder caused by the induction of new defect occurs in the composition with minimum amount of doping atoms. This effect is consistent with the the largest WAT amplitude (Fig. 1), registered for the composition $Bi_{1.5}(As_2S_3)_{98.5}$. This could also be an explanation for the significant change in the optical band gap in comparison to the matrix band gap (Table I). In terms of chemical bonds, it can be assumed that dopant atoms in this concentration form the bridge-like bonds with sulphur atoms, hence increasing the structural disorder. With further increase of Bi content, parameter E_e converges to the matrix value. It all indicates that at the lowest concentration there are special effect associated with the nanocluster structure. For higher dopant content, Bi will be substituted and incorporated in As_2S_3 matrix.

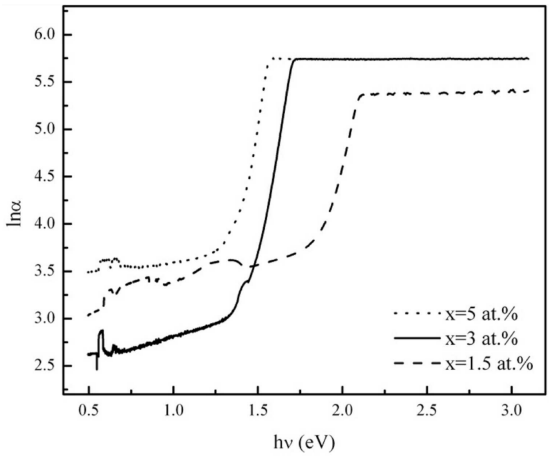

Fig. 3. Dependence of $\ln\alpha$ on $h\nu$ of glassy $Bi_x(As_2S_3)_{100-x}$ system.

The Raman spectroscopy of $Bi_{1.5}(As_2S_3)_{98.5}$ and $Bi_3(As_2S_3)_{97}$ chalcogenides was made to study modifications in structure influenced by bismuth doping. The recorded spectra, shown in Fig. 4, clearly indicate a significant presence of realgar phase in the network structure of the glass with $x = 1.5$ at.% of Bi (peaks at 135, 145, 165, 185, 220, and 361 cm^{-1}) [19], that is, the existence of nanophase separation. On the other hand, it can be noticed that for the sample with $x = 3$ at.% intensities of Bi peaks attributed to the vibration of Bi_2S_3 structural unit (185, 232, and 270 cm^{-1}) [20] increase, indicating that the share of realgar phase decreases. The peaks at 310, 340, and 380 cm^{-1} observed for both samples correspond to the vibrations of structural unit As_2S_3 [21].

The refractive index dispersion curves of the samples are plotted in Fig. 5 and show usual dispersion behavior. They also indicate increase of the refractive index n with Bi content and typical values for chalcogenide glasses.

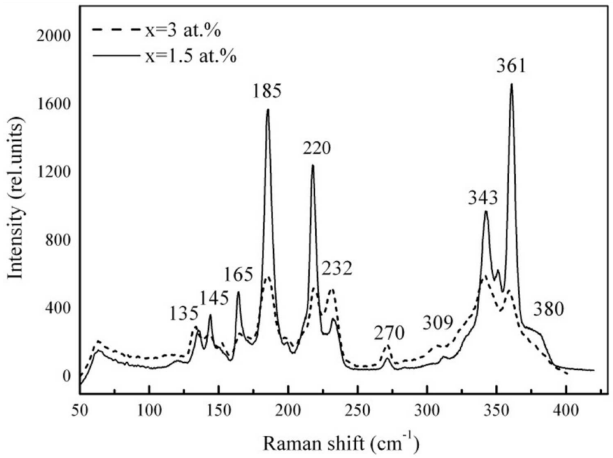

Fig. 4. Raman spectra of glassy $Bi_x(As_2S_3)_{100-x}$ system.

The application of the Wemple–DiDomenico model (WDD) [22] for the analysis of the refractive index behavior in the transparent region is given in Fig. 6. This dispersion model establishes the relation between the refractive index and the strength of the oscillator A ($A = E_d/E_0$) as follows:

$$n^2 = 1 + \frac{E_d E_0}{E_0^2 - E^2}, \tag{4}$$

where E denotes the energy of incident photons, E_0 is the effective energy of oscillator and E_d is a dispersion parameter, which indicates the strength of optical interband transitions. Experimental data fitting is illustrated in Fig. 6, and the numerical values are summarized in Table II.

TABLE II

The Wemple DiDomenico parameters of glassy $Bi_x(As_2S_3)_{100-x}$ system.

x [at.%]	E_0 [eV]	E_d [eV]	A	n_0	ν_0 [10^{15} Hz]
1.5	4.82 (5)	24.49 (6)	5.08 (5)	2.47 (3)	1.17 (2)
3	4.78 (5)	25.55 (9)	5.34 (9)	2.52 (6)	1.16 (5)
5	4.73 (4)	27.55 (8)	5.82 (7)	2.61 (4)	1.15 (3)

The relation between the parameter E_d and the changes in the structure of glass network is illustrated with empirical equation

$$E_d = \beta N_c Z_a N_e, \tag{5}$$

where $\beta = 0.37 \pm 0.04$ eV [23] in case of covalent bonding

(dominant in chalcogenide glasses), N_c is the coordination number of nearest cationic neighbors of anions, Z_a is the formal valence of the anion and N_e is the effective number of valence electrons per anion.

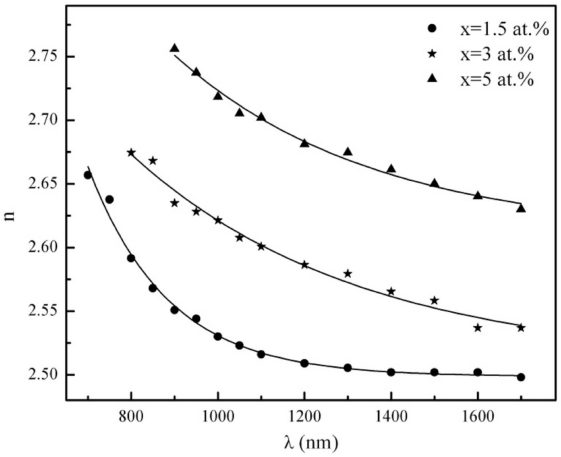

Fig. 5. Dispersion of refractive index of glassy $Bi_x(As_2S_3)_{100-x}$ system.

The parameters from Eq. (4) (the effective energy of oscillator E_0 and dispersion parameter E_d) are obtained by fitting the experimental data. Given the parameter E_0 corresponds to the distance between the "centers of gravity" of valence and conduction bands, its decrease with the higher impurity atoms content indicates the agreement of WDD analysis with the results of spectroscopic measurements (Table I).

Considering that the energy of effective oscillator is associated with the energy of various chemical bonds in the investigated material [24], the reduction of E_0 may be explained by the formation of new structural units of Bi–S type with a lower binding energy (315.5 kJ/mol), replacing the As–S bonds (379.5 kJ/mol) [25]. Regarding the dispersion parameter E_d values (Table II), one concludes that the introduction of Bi in As_2S_3 matrix increases the strength of the optical interband transitions. Following Eq. (5), N_c and N_e parameters have the dominant influence on the oscillator strength. The increase of the static refractive index as a function of Bi content is in accordance with the absorption edge shift toward lower frequencies (Fig. 1). It should also be noted that the frequencies of the oscillator expectedly fall in the UV region of the spectrum.

WDD analysis also enabled the calculation of the static refractive index $n_\infty = \sqrt{1 + E_d/E_0}$ and the mean frequency of electron oscillator $\nu_0 = c/\lambda_0 d$. The obtained values are given in Table II.

Applying WDD model for the description of refractive index dispersion of investigated glasses also enabled the establishment of correlation between linear and nonlinear optical quantities. The nonlinear refractive index values of glassy quasibinary system Bi–As_2S_3 are calucated from the Fournier and Snitzer equation [26]:

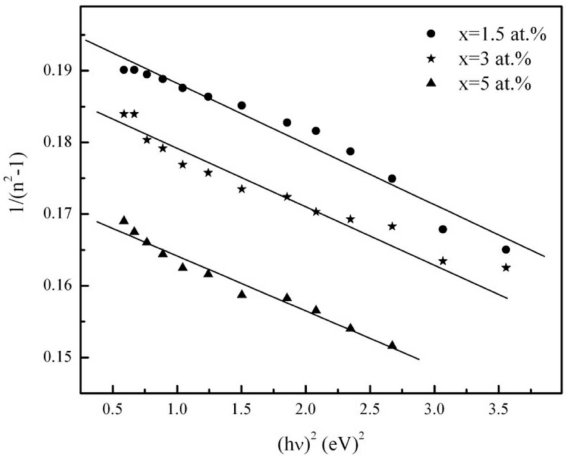

Fig. 6. Dependence of $1/\left(n^2-1\right)$ on $(h\nu)^2$ of glassy $Bi_x(As_2S_3)_{100-x}$ system.

$$n_2 = \frac{(n^2+2)^2(n^2-1)E_d}{4\pi n N (E_0)^2}, \tag{6}$$

where N is the number of atoms per volume.

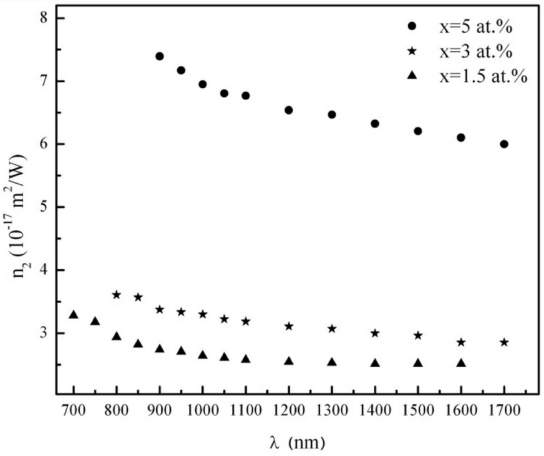

Fig. 7. Dispersion of nonlinear refractive $(h\nu)^2$ of glassy $Bi_x(As_2S_3)_{100-x}$ system.

The calculated values are represented as a dispersion curve in Fig. 7. According to the results illustrated in Fig. 7, the nonlinearity significantly increases with the content of impurity atoms. The nonlinear refractive index n_2 exhibits analogous dispersion behavior as the linear refractive index n (Fig. 5). Also, n_2 of investigated materials in this paper is higher by two orders of magnitude in comparison to As_2S_3 [27], and even four orders of magnitude in comparison to pure silica [28, 29]. According to the spectroscopic results (Table I) and the Moss rule [30] this can be explained as the consequence of reducing of the optical gap with Bi atoms introduction. Moreover, due to the large nonlinearity, the lower power and shorter interaction lengths are required for possible applications. The values of nonlinear refractive index of about 10^{-17} m^2/W could indicate the potential applicability of the investigated glasses in telecommunication

devices that operate on $\lambda \approx 1.5$ μm. Given that the peaks in the energy spectrum of the nonlinear refractive index and nonlinear absorption in amorphous semiconductors occur at 0.5–0.9E_g [31], the materials having the optical band gap in the range of 1.0–1.6 eV feature optimal values of nonlinear parameters. However, the practice has shown that the materials with a slightly larger optical band gap ($E_g \approx 1.8$ eV) and $n_2 \approx 10^{-17}$ m^2/W satisfy the requirements for applications in telecommunication devices [32], which is explained by the existence of energy states in the tails of valence and conductive band, limiting the optical transparency. Thus, the systems under investigation may be used as optical materials for high speed communication fibers and also in optical limiting devices.

4. Conclusion

The analysis of the absorption coefficient dispersion curves have shown that the weak absorption tail amplitude decreases and the absorption edge shifts to the lower energies as a function of Bi content. The reduction in the optical band gap is also found. Based on the tail width estimation of the localized states and the Raman spectra analysis, it was concluded that the effect of doping on the structural disorder is the largest for the minimum concentration of the introduced bismuth atoms ($x = 1.5$ at.%). The substitution and consequently incorporation of dopant atoms into the structural units of matrix starts with increase of the dopant atoms content. The analysis of the refractive index of studied glasses show normal dispersion and increasing trend of parameter n with Bi content. We have shown the agreement of the Wemple–di Domenico dispersive model with our spectroscopic measurements. Obtained results for nonlinear refractive index may be the path toward more sensitive optical limiting devices, indicating potential use of these glasses as optical materials for high speed communication fibers.

Acknowledgments

Authors acknowledge the financial support of the Ministry of Science, Education and Technological Development of the Republic of Serbia (projects ON 171022 and III 45020) and the financial support of the Provincial Secretariat for Higher Education and Scientific Research, Autonomous Province of Vojvodina (project No. 114-451-1745/2016).

References

[1] R.K. Brow, *J. Non-Cryst. Solids* **263**, 1 (2000).

[2] R.A.H. El-Mallawany, *Tellurite Glasses Handbook: Physical Properties and Data*, CRC Press, Boca Raton (FL) 2002.

[3] J. Eggleton, B. Luther-Davies, K. Richardson, *Nat. Photon.* **5**, 141 (2011).

[4] C. Conseil, Q. Coulombier, C. Boussard-Plédel, J. Troles, L. Brilland, G. Renversez, D. Mechin, B. Bureau, J.L. Adam, J.J. Lucas, *J. Non-Cryst. Solids* **357**, 2480 (2011).

[5] J. Keirsse, B. Bureau, C. Boussard-Pledel, P. Leroyer, M. Ropert, V. Dupont, M.L. Anne, C. Ribault, O. Sire, O. Loreal, J.L. Adam, *Proc. SPIE* **5459**, 61 (2004).

[6] F. Désévédavy, G. Renversez, J. Troles, P. Houizot, L. Brilland, I. Vasilief, Q. Coulombier, N. Traynor, F. Smektala, J.L. Adam, *Opt. Mater.* **32**, 1532 (2010).

[7] A.A.M. Andriesh, M.S. Iovu, S.D. Shutov, *J. Optoelectron. Adv. Mater.* **4**, 631 (2002).

[8] A.V. Kolobov, J.J. Tominaga, *J. Optoelectron. Adv. Mater.* **4**, 679 (2002).

[9] M.V. Šiljegović, G.R. Štrbac, F.N. Skuban, S.R. Lukić-Petrović, *J. Therm. Anal. Calorim.* **105**, 947 (2011).

[10] S.J. Skuban, S.R. Lukić, I.O. Gúth, D.M. Petrović, *J. Optoelectron. Adv. Mater.* **4**, 737 (2002).

[11] J. Tauc, *J. Non-Cryst. Solids* **97-98**, 149 (1987).

[12] J.M. Gonzalez-Leal, R. Prieto-Alcon, J.A.A. Angel, E. Marquez, *J. Non-Cryst. Solids* **315**, 134 (2003).

[13] J. Fournier, E. Snitzer, *IEEE J. Quant. Electron.* **10**, 473 (1974).

[14] D.L. Wood, J. Tauc, *Phys. Rev. B* **5**, 3144 (1972).

[15] Y. Kanamori, S. Terunuma, T. Takahashi, J. Miyashita, *Lightwave Technol.* **2**, 607 (1984).

[16] M. Popescu, A. Andriesh, V. Chumash, M. Iovu, S. Shutov, D. Tsiuleanu, *The Physics of Chalcogenide Glasses*, Stiintifica Bucharest, I.E.P. Stiinta, Chisinau 1996.

[17] N.F. Mott, E.A. Davis, *Electronic Processes in Non-Crystalline Materials*, Clarendon Press, Oxford 1979.

[18] K. Hachiya, *J. Non-Cryst. Solids* **321**, 217 (2003).

[19] D. Vanderbilt, J. Joannopoulos, *Phys. Rev. B* **23**, 2596 (1981).

[20] M.A. Majeed Khan, M. Zulfequar, M. Husain, *Opt. Mater.* **22**, 21 (2003).

[21] R. Zallen, M.L. Slade, *Phys. Rev. B* **18**, 5775 (1978).

[22] J.S. Lannin, J.M. Calleja, M. Cardona, *Phys. Rev. B Condens. Matter* **12**, 585 (1975).

[23] A.R. Kampf, R.T. Downs, R.M. Housley, R.A. Jenkins, J. Hyršl, *Mineral. Mag.* **75**, 2857 (2011).

[24] S.H. Wemple, M. DiDomenico, *Phys. Rev. B* **3**, 1338 (1971).

[25] E. Márquez, A.M. Bernal-Oliva, J.M. González-Leal, R. Prieto-Alcón, T. Wagner, *J. Phys. D Appl. Phys.* **39**, 1793 (2006).

[26] *Handbook of Chemistry and Physics*, Ed. R.C. Weast, CRC Press, Cleveland 1974.

[27] M. Asobe, T. Kanamori, K. Kubodera, *IEEE J. Quant. Electron.* **29**, 2325 (1993).

[28] S. Smolorz, F. Wise, N.F. Borrelli, *Opt. Lett.* **24**, 1103 (1999).

[29] A. Boskovic, S.V. Chernikov, J.R. Taylor, K.L. Gruner-Nielsen, O.A. Levring, *Opt. Lett.* **21**, 1966 (1996).

[30] T.S. Moss, *Phys. Status Solidi B* **131**, 415 (1985).

[31] K. Tanaka, *J. Mater. Sci.* **16**, 633 (2005).

[32] K. Ogusu, J. Yamasaki, S. Maeda, M. Kitao, M. Minakata, *Opt. Lett.* **29**, 265 (2004).